

Nonparametric Bayesian sparse graph linear dynamical systems: supplementary material

Rahi Kalantari, Joydeep Ghosh, and Mingyuan Zhou

A Proof of Lemma 1

Proof. Since $z_{ij} \leq m_{ij}$ by construction, we have

$$\begin{aligned} \mathbb{E}[\|\mathbf{Z}\|_0] &\leq \mathbb{E}\left[\sum_{i=1}^{\infty}\sum_{j=1}^{\infty}m_{ij}\right] = \mathbb{E}\left[\sum_{i=1}^{\infty}\sum_{j\neq i}r_i r_j + r_0\sum_{j=1}^{\infty}r_j\right] \\ &= \mathbb{E}\left[G^2 - \sum_{k=1}^{\infty}r_k^2 + r_0 G\right]. \end{aligned} \quad (7)$$

Following Lemma 1 of Zhou (2015), it is straightforward to show that the right hand side of (7) is the same as that of (4) in main article. \square

B MCMC Convergence and Complexity Analysis

We show in Figure C.1 the trace plots of four representative model parameters, including two weight components of the gamma process r_i , the number of inferred nodes, and the total number of edges. The plots are obtained by running the model on the Beijing meteorological data. They show that the proposed Gibbs sampling algorithm converges fast and mixes well. Each Gibbs sampling iteration of the SGLDS has a complexity of $\mathcal{O}(KP^3 + K + N_Z + K^2 + TK^3)$, where T is the length of observed time series, K is the latent dimension of \mathbf{x}_t , N_Z is the number of non-zero elements in the transition matrix $(\mathbf{W} \odot \mathbf{Z})$, and P is the dimension of the observation. By contrast, a vanilla LDS has a sampling complexity of $\mathcal{O}(K + K^2 + TK^3 + KP^3)$. Considering that $N_Z < K^2$, we can conclude that our algorithm does not notably increase the complexity of the sampling algorithm.

C Additional figures

Shown in Figure C.2 is the graphical representation of our model.

Figure C.3 shows that the loops within the inferred sparse random graph capture the seasonal components of the time series. Note different loops could have overlapping nodes.

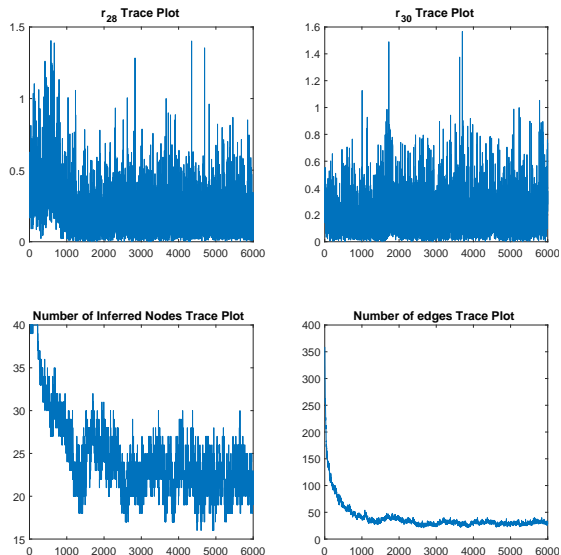


Figure C.1: Trace plots of four different model parameters.

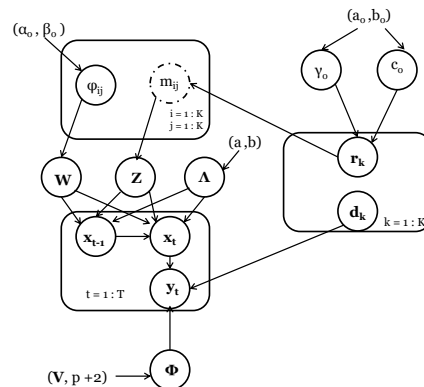


Figure C.2: Graphical Model

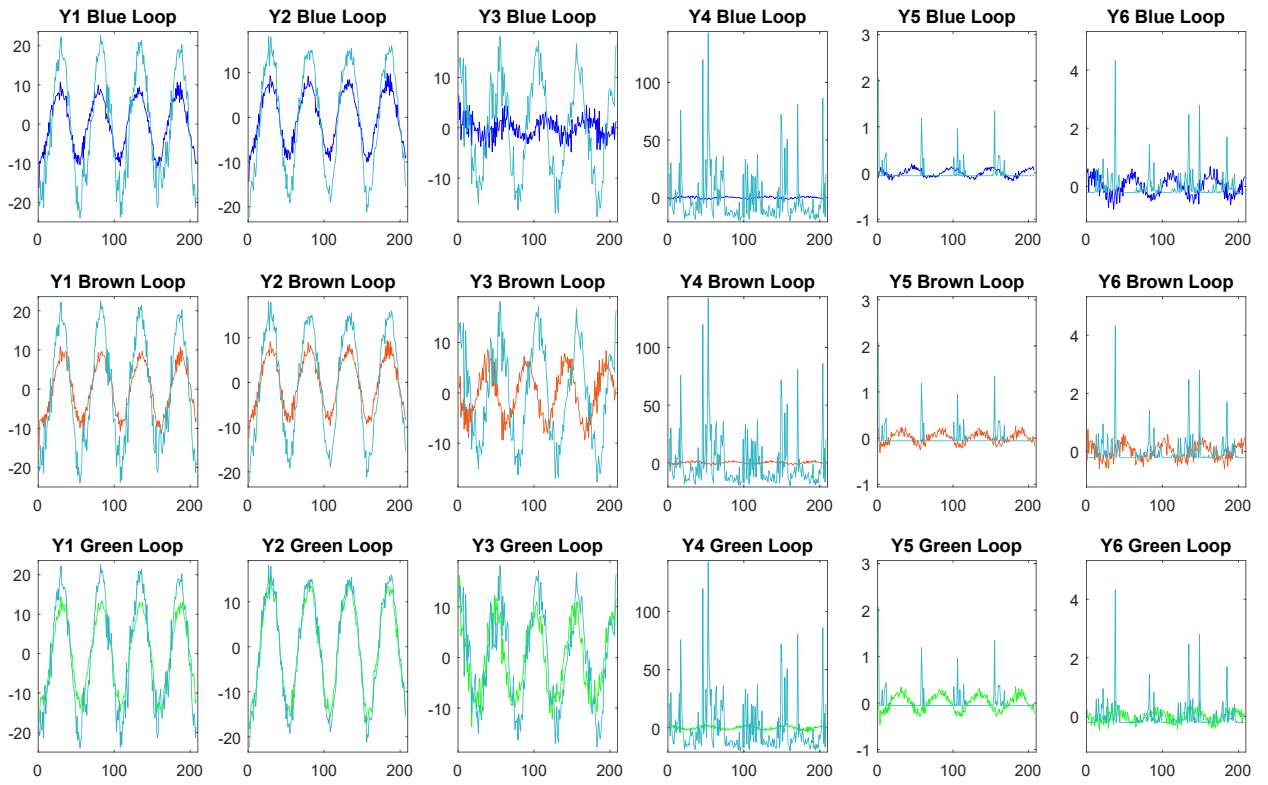


Figure C.3: The six-dimensional time series of the Beijing meteorological data and the reconstructed components using the states belonging to loop 1, 2, or 3 shown in Figure 2.